MOLECULAR AND CELLULAR BIOLOGY, Oct. 2006, p. 7201–7210 Vol. 26, No. 19
0270-7306/06/$08.00+0 doi:10.1128/MCB.00459-06

Disruption of Ledgf/Psip1 Results in Perinatal Mortality and Homeotic Skeletal Transformations

Heidi G. Sutherland,[1]* Kathryn Newton,[1]† David G. Brownstein,[2] Megan C. Holmes,[3] Clémence Kress,[1] Colin A. Semple,[1] and Wendy A. Bickmore[1]

MRC Human Genetics Unit, Crewe Road, Edinburgh EH4 2XU, United Kingdom[1]; Research Animal Pathology Core Facility, Queen's Medical Research Institute, Edinburgh University, Edinburgh EH16 4TJ, United Kingdom[2]; and Endocrinology Unit, Centre for Cardiovascular Science, Queen's Medical Research Institute, Edinburgh University, Edinburgh EH16 4TJ, United Kingdom[3]

Received 16 March 2006/Returned for modification 25 April 2006/Accepted 24 June 2006

PC4- and SF2-interacting protein 1 (Psip1)—also known as lens epithelium-derived growth factor (Ledgf)—is a chromatin-associated protein that has been implicated in transcriptional regulation, mRNA splicing, and cell survival in vitro, but its biological function in vivo is unknown. We identified an embryonic stem cell clone with disrupted *Psip1* in a gene trap screen. The resulting Psip1-βgeo fusion protein retains chromatin-binding activity and the PWWP and AT hook domains of the wild-type protein but is missing the highly conserved C terminus. The majority of mice homozygous for the disrupted *Psip1* gene died perinatally, but some survived to adulthood and displayed a range of phenotypic abnormalities, including low fertility, an absence of epididymal fat pads, and a tendency to develop blepharitis. However, contrary to expectations, the lens epithelium was normal. The mutant mice also exhibited motor and/or behavioral defects such as hind limb clenching, reduced grip strength, and reduced locomotor activity. Finally, both *Psip1*$^{-/-}$ neonates and surviving adults had craniofacial and skeletal abnormalities. They had brachycephaly, small rib cages, and homeotic skeletal transformations with incomplete penetrance. The latter phenotypes suggest a role for Psip1 in the control of *Hox* expression and may also explain why PSIP1 (LEDGF) is found as a fusion partner with NUP98 in myeloid leukemias.

PC4- and SF2-interacting protein 1 (Psip1) has been isolated in a number of independent experimental settings and has been assigned a variety of names and putative functions. *Psip1* encodes two protein isoforms with molecular masses of 52 and 75 kDa. p52 and p75 were identified as interacting with transcription factor PC4 and shown to act as transcriptional coactivators (8). p75 is also referred to as lens epithelium-derived growth factor (LEDGF) since it was identified as a cell survival factor under a variety of conditions of environmental stress, and it has been implicated as a transcriptional regulator of stress-related genes (32). PSIP1 (LEDGF) is also a nuclear autoantigen targeted by autoantibodies in some patients with atopic dermatitis and other inflammatory conditions involving dysregulated apoptosis. It is thought to exert an antiapoptotic effect by transcriptional activation of stress-related genes (7), and it is cleaved by caspases (38).

Psip1 has been reported to localize to chromatin in both interphase and mitotic chromosomes (27, 28, 35, 37). The N-terminal domain of Psip1 contains a PWWP domain (Fig. 1B), a member of the Tudor domain "royal family" that includes chromo domains—some of which are known to bind to chromatin (24). There are conflicting data on the ability of the Psip1 PWWP domain to bind to free DNA in vitro (33, 36). The PWWP domain of the DNA methyltransferase Dnmt3b is required for targeting the protein to chromatin and chromosomes (2, 10), and the Psip1 PWWP domain also affects the interaction of the protein with chromatin in vivo (36). Psip1 also contains AT hook-like motifs (Fig. 1B), and some of these have been implicated in DNA binding in vitro (36).

Apart from its suggested role as a transcriptional regulator (21, 32), an integrase-binding domain (IBD) in p75/PSIP1 tethers human immunodeficiency virus type 1 integrase to host chromosomes and so prevents integrase degradation (3, 4, 23, 37) (Fig. 1B). This is important for retroviral integration (5) and replication (6), but the normal cellular role of the IBD is unknown.

Most assays for normal Psip1 function have involved overexpression of the protein in cultured cells. Apart from the role in tethering viral integrase, depletion of PSIP1 from cells in culture by RNA interference reveals no obvious cellular phenotype (5, 6, 22); therefore, the biological function of PSIP1 remains unknown.

We originally identified Psip1 as a chromosomally associated protein during the course of a gene trap screen to identify novel murine nuclear and chromosomal proteins (35). Two independent gene-trapped clones were obtained, one in mouse F9 embryonal carcinoma cells and the other in mouse embryonic stem (ES) cells (Fig. 1). Here we have used the disrupted *Psip1* (*Ledgf*) gene from the trapped ES cell clone to generate mutant mice and to investigate the resulting biological phenotype. While the majority of mice with disrupted *Psip1* died perinatally, some survived to adulthood and displayed complex phenotypic abnormalities, including fertility and motor defects. However, significantly, given the association of Psip1

* Corresponding author. Mailing address: MRC Human Genetics Unit, Crewe Road, Edinburgh EH4 2XU, United Kingdom. Phone: (44) 131 332 2471. Fax: (44) 131 467 8456. E-mail: H.Sutherland@hgu.mrc.ac.uk.

† Present address: Clinical Research Division, Fred Hutchinson Cancer Research Center, Seattle, WA 98109.

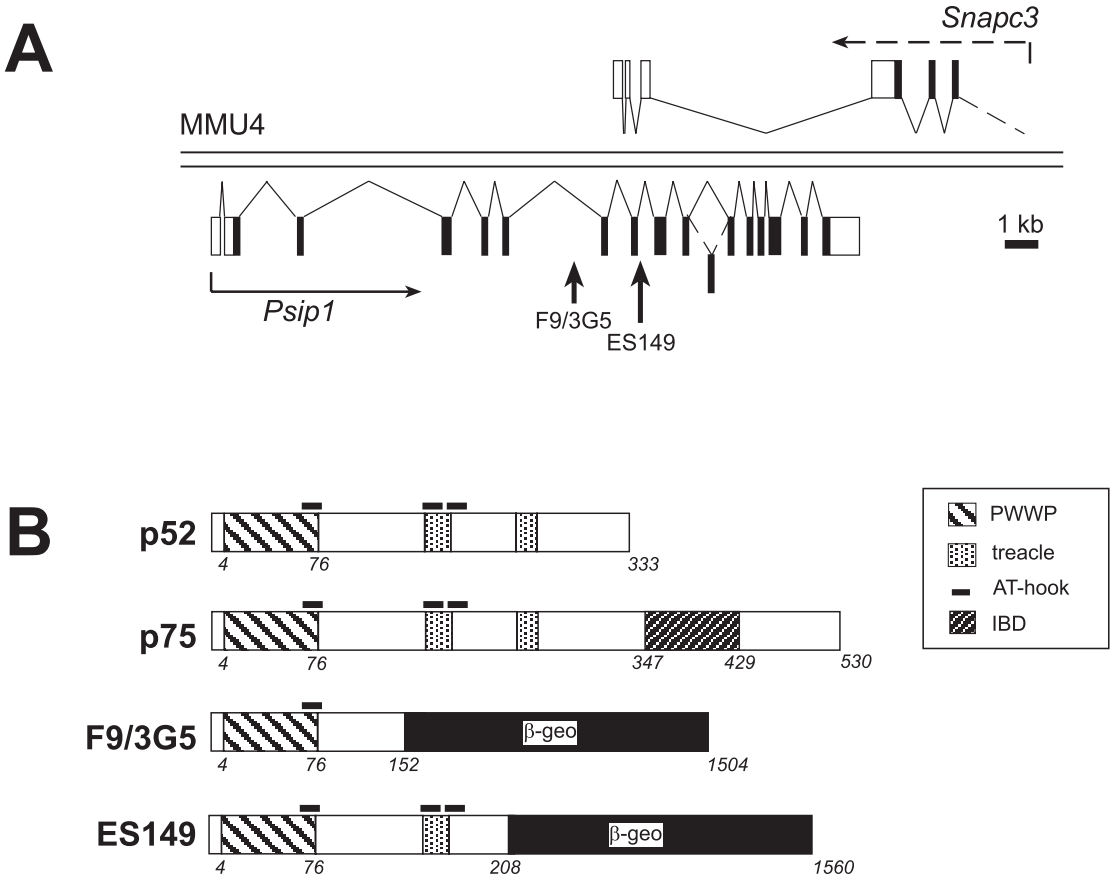

FIG. 1. Gene trap disruption of the *Psip1* locus. (A) Predicted intron-exon structure of mouse *Psip1* and antisense *Snapc3* with integration sites of the F9/3G5 and ES149 gene trap lines indicated. (B) Diagram of the Psip1 p52 and p75 protein isoforms and the predicted gene trap fusion proteins in F9/3G5 and ES149 gene trap lines. Known protein motifs predicted by SMART/PFAM and the experimentally determined human immunodeficiency virus IBD are depicted.

(LEDGF) with growth of the lens epithelium in vitro, *Psip1*$^{-/-}$ mice had a normal lens epithelium. Both *Psip1*$^{-/-}$ neonates and surviving adults also had brachycephaly, small rib cages, and homeotic skeletal transformations similar to those seen in mice with mutations in *Hox* genes or components of the PRC1 polycomb complex. Therefore, proteins encoded by *Psip1* may function in the control of *Hox* gene expression. This would also be consistent with the finding of human PSIP1 (LEDGF) as a fusion partner with NUP98 in myeloid leukemias (11, 15). The other recurrent leukemia-associated fusion partners of NUP98 are encoded by *Hox* genes themselves (1).

MATERIALS AND METHODS

Cell culture and immunostaining. The F9 and ES cell *Psip1* gene trap lines (WF9/3G5 and ES149) were generated, maintained, and immunostained with an antibody against β-galactosidase (β-gal; Europa) as previously described (35).

Generation of p75 antibodies. A fragment of human p75/Psip1 from amino acid 326 to amino acid 529 encompassing the whole of the p75-specific region (Fig. 1B) was generated by PCR with primers 5′ ACTGGATCCCAGCAGAA TAAAGATGAAGG 3′ and 5′ TAGTAAGCTGATCTAGTGTAGAATCCT TCAG 3′, fused in frame in pET-32a, and expressed in *Escherichia coli* [BL21-CodonPlus(DE3)-RP; Stratagene] to produce a fusion protein with thioredoxin and a His tag. Fusion protein was purified on a nickel-agarose column and used to immunize sheep (Scottish Diagnostics). For antibody affinity purification, the same fragment of p75 was fused in frame with glutathione *S*-transferase in pGEX 4T-1, purified on glutathione-agarose, and then immobilized on a cyanogen bromide-activated Sepharose 4B column (Pharmacia). Serum from the fourth bleed was diluted in phosphate-buffered saline, filtered, and put over the column three times. The column was then washed with 20 bed volumes of high-salt wash buffer (10 mM Tris-Cl [pH 7.5], 500 mM NaCl), followed by 50 bed volumes of phosphate-buffered saline. Antibody was eluted with 100 mM glycine (pH 2.7)–150 mM NaCl–10% glycerol into 1 M Tris-HCl (pH 8.8) for neutralization. Protein-containing fractions were pooled and concentrated with a Centricon 30 column (Millipore), the concentration was estimated from the A_{280}, and the antibody was stored at −80°C in 20% glycerol.

Generation and genotyping of *Psip1* mutant mice. The ES149 cell line was a gene trap of E14 ES cells (35), which are derived from the mouse substrain 129/Ola. ES149 cells were passaged the day before injection into blastocysts collected at 3.5 days postcoitum (dpc) from superovulated C57BL/6 females and transferred into pseudopregnant recipient females. Chimeric pups were identified by their agouti coat color and, when mature, were mated to both MF1 outbred and C57BL/6 mice. Two male chimeras yielded germ line transmission, and heterozygotes for the *Psip1* mutation were identified by Southern blot analysis for presence of the *lacZ* portion of the gene trap vector. Heterozygotes obtained from crosses with either MF1 or C57BL/6 mice (termed first backcross) were backcrossed with wild-type (WT) mice from each respective strain at least three more times before matings between heterozygotes were set up.

DNA for genotyping of mice was obtained from tail tips or ear punches. To detect the presence of the gene trap vector (SA-βgeo construct) by Southern blotting, genomic DNA was digested with EcoRI and hybridized with a dCTP-p32-labeled probe 3-kb BamHI fragment encompassing *lacZ*. More routinely, mice were genotyped by testing for *lacZ* by PCR with primers 5′ GTTGCGCA GCCTGAATGGCG 3′ and 5′ GCCGTCACTCCAACGCAGCA 3′, which generate a 432-bp PCR fragment. To genotype offspring from *Psip1* heterozygous (+/−) crosses, HindIII-digested genomic DNA was analyzed by Southern blot-

ting with a 223-bp PCR product generated from exon 9 of *Psip1* (5′ GGTTAT TGATGAAGATAAAAG 3′ and 5′ TTCACCCTCTTGATCGTCTTC 3′). Alternatively, genomic DNA was analyzed by PCR for the presence of both *lacZ* as described above and the endogenous *Psip1* locus with primers from introns 8 and 9 (5′ CTGATGAGAGATTGGAGGAGG 3′ and 5′ CTGCAAATGCCAAGG GACATG 3′) into which the gene trap construct was inserted. An 860-bp PCR product is generated from the WT locus, but no product is obtained from the gene-trapped locus.

Analysis of *Psip1* expression in mice generated from the ES149 gene trap line. Embryos obtained at 14.5 dpc from a cross between male and female *Psip1*$^{+/-}$ mice were stored at −80°C after a biopsy was taken for genotyping each individual. For analyzing mRNA, half of an embryo for each genotype was homogenized in TriReagent (Sigma) and the RNA was extracted according to the manufacturer's instructions. After DNase I treatment of the RNA, reverse transcription (RT)-PCRs were performed with primers for *Psip1* (5′ AGATGCAT AGAGGCCCTGGATG 3′ and 5′ ACATCTGAAGCTGCCGACCTAG 3′), which generate a 499-bp product from beyond the site of gene trap integration in the transcript, and *Snapc3* (5′ TGAGCACATCAGCAAAGACCTC 3′ and 5′ AGGTTCCTGGGTCAACATAAGG 3′), which generate a 511-bp product—to check the transcript from the opposite strand, and a 70-bp product of *Gapdh* (5′ CTCAAGATTGTCAGCAATGCA 3′ and 5′ CCTTCCACAATGCCAAAGTT 3′) was used as a positive control.

For protein analysis, the other half of the embryo was homogenized in sodium dodecyl sulfate loading buffer and the samples were boiled and sonicated. Aliquots were subjected to 10% sodium dodecyl sulfate-polyacrylamide gel electrophoresis and Coomassie staining to estimate protein concentrations. Samples with equal amounts of protein were run and transferred to HybondP (Amersham) membranes. Immunodetection was performed with the sheep p75-specific antibody described above (1:1,000 dilution), an anti-sheep antibody–horseradish peroxidase conjugate (Jackson Labs), and chemiluminescence. Embryos from timed matings were harvested and stained with 5-bromo-4-chloro-3-indolyl-β-D-galactopyranoside (X-Gal) as described elsewhere (26).

Pathology and histochemistry. Neonatal mice were humanely killed by decapitation, and thoracoabdominal organs and heads were fixed in 10% neutral buffered formalin and processed for histopathology. Thoracoabdominal organ blocks were serially sectioned parallel to the sagittal plane at 4 μm. Fifty evenly spaced sections spanning the entire block were stained with hematoxylin and eosin (H&E). Heads were serially sectioned transversely, and 25 evenly spaced sections spanning the entire block were stained with H&E. Adult mice were humanely killed with CO_2 gas. The initial group (two *Psip1*$^{-/-}$ and four *Psip1*$^{+/-}$ mice) received detailed gross and histopathological examination of all organ systems. A second group (two *Psip1*$^{-/-}$, two *Psip1*$^{+/-}$, and two WT mice) received a detailed gross examination and histopathological examination of the adrenal gland, kidney, eyelid, and stomach. Tissues were fixed in 10% neutral buffered formalin and wax embedded, and 4-μm sections were stained with H&E. Alizarin red-alcian blue staining of adult and newborn mice was performed as described previously (29). Briefly, animals were skinned, eviscerated, and fixed in 95% ethanol. They were then transferred to acetone for 2 days and then stained with alizarin red-alcian blue (Sigma) for 3 days at room temperature, subsequently cleared with 1% KOH, and finally stored in glycerol.

Behavioral and motor function studies. In hind limb extension tests, mice were suspended by their tails and the extent of hind limb extension was observed. If both hind limbs showed the extension reflex, including splayed toes, the mouse was considered normal. If the toes and one or two hind limbs were clenched to the body, the mouse was considered to fail the test. In grip strength tests, mice were suspended from a pencil with their forepaws. A mouse that was not able to suspend itself for any amount of time was considered to fail this test. In open-field tests, mice were placed in an open-field box (60 by 60 cm) marked off into 25 equal squares. Tests were videotaped or captured by a computer tracking program (Limelight; Actimetrics) to allow full analysis. The outer row of squares adjacent to the walls of the field are considered less anxiogenic than the inner squares. For 5 min, the number of crossings, time, and distance (movement of all four legs into a new square) into each square was noted together with other ethological parameters such as the numbers of rearings and fecal boli. Total movement in the field reflects general activity, and relative movement into the inner zone correlates with the anxiety state of the mouse.

RESULTS

Gene-trapped forms of Psip1 are missing conserved domains of the protein but still retain chromatin-binding activity. We previously performed a gene trap screening of mouse cells to identify nuclear proteins and characterize their distribution within the nucleus (35). We obtained a number of clones in which the resulting βgeo fusion protein was found to associate with chromosomes. In two independent clones obtained (one in F9 embryonal carcinoma cells and the other in E14 ES cells), the gene that had been trapped was identified as *Psip1*. The sites of integration of the gene trap vector in the F9/3G5 and ES149 cell lines are shown in Fig. 1A. In F9/3G5, the gene trap vector was integrated into the intron between exons 6 and 7 of *Psip1*, whereas in ES149 insertion occurred between exons 8 and 9. This results in fusion proteins that encode the N-terminal 152 or 208 amino acids of Psip1, respectively, fused to the βgeo reporter (Fig. 1B). These proteins are expressed under the control of the endogenous *Psip1* promoter but are missing C-terminal functional protein domains (Fig. 1B). For example, one or two of the treacle motifs have been removed by the ES149 and F9/3G5 integrations, respectively. These are highly polar motifs that feature in the nucleolar protein treacle, which is mutated in Treacher Collins syndrome, an autosomal dominant disorder of craniofacial development (16). The IBD is also removed by both gene traps.

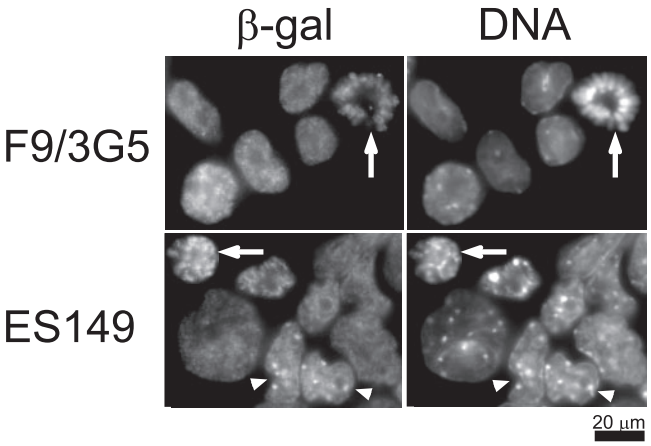

FIG. 2. Subcellular localization of Psip1-βgeo fusion proteins. Shown is immunostaining of F9/3G5 and ES149 cells with an anti-β-gal antibody showing localization of the Psip1–β-geo fusion proteins in the nuclei and on chromosomes in mitotic cells (arrows). In some ES149 nuclei, the fusion protein is concentrated at the DAPI-bright heterochromatic foci (arrowheads).

Psip1 is highly conserved among vertebrates over the known protein motifs shared by both the p52 and p75 isoforms but also the IBD and other p75-specific sequences in the C-terminal end of the protein that are lost in the F9/3G5 and ES149 gene traps. Hence, it is likely that the gene-trapped proteins have perturbed function.

With an antibody against β-gal that detects the βgeo portion of the gene-trapped proteins, we found that the Psip1 fusion proteins in both gene trap clones localize to interphase nuclei and to mitotic chromosomes (Fig. 2). In ES149 cells, the fusion protein could sometimes be seen to colocalize with the brightly 4′,6′-diamidino-2-phenylindole (DAPI)-stained foci of pericentric heterochromatin that are easily observed in mouse cells (35). This was not seen in F9/3G5 cells and may reflect the loss of additional AT hook domains in this case (Fig. 1B). AT

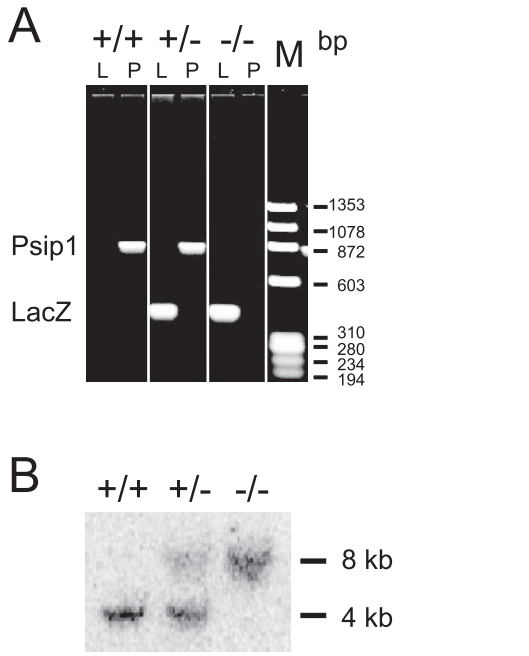

FIG. 3. Genotyping of ES149 mice for gene trap disruption of *Psip1*. (A) PCR analysis of WT (+/+) and heterozygous (+/−) and homozygous (−/−) *Psip1* mutant mice with primers for *lacZ* (L) (432-bp band) and endogenous *Psip1* (P) (860-bp band). (B) Southern blot analysis of HindIII-digested genomic DNA from +/+, +/−, and −/− mice probed with a PCR product for exon 9 of *Psip1*. This results in a 4-kb band for the endogenous *Psip1* locus and an 8-kb band for the gene-trapped locus.

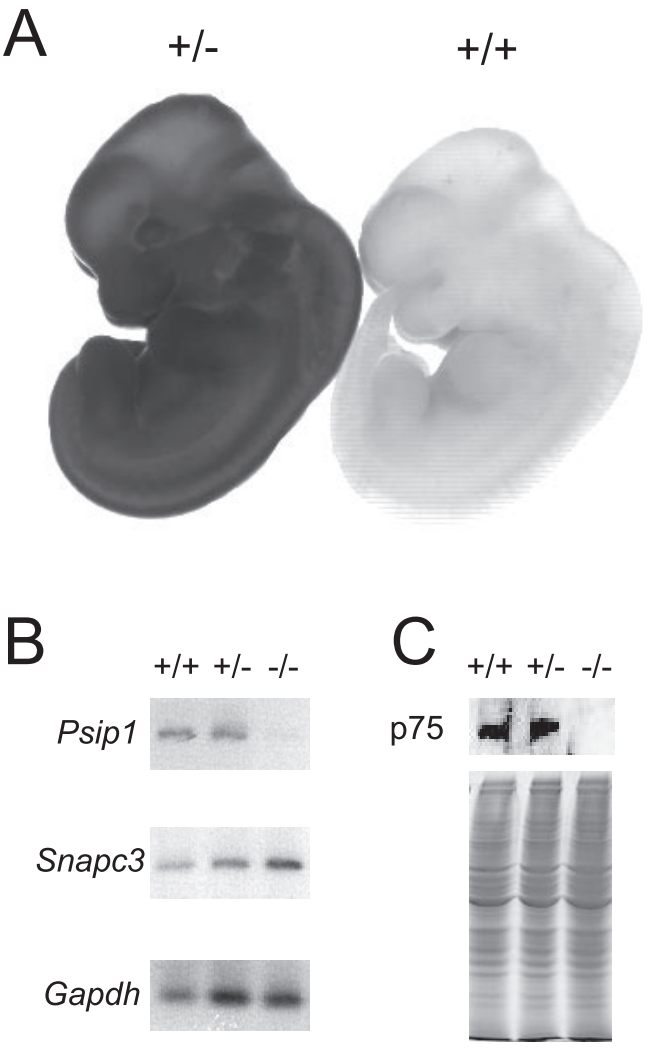

FIG. 4. *Psip1* expression in WT and mutant mice. (A) X-Gal staining of WT and *Psip1*$^{+/-}$ embryos at 11.5 dpc. (B) RT-PCR analysis of *Psip1* and *Snapc3* mRNAs in *Psip1*$^{+/+}$, *Psip1*$^{+/-}$, and *Psip1*$^{-/-}$ mice. *Gapdh* was used as a control. (C) Western blot analysis of p75/Psip1 in protein extracts form +/+, +/−, and −/− embryos (top). The Coomassie-stained polyacrylamide gel at the bottom shows protein loading.

hooks are known to bind preferentially to AT-rich sequences, such as those found in pericentric heterochromatin, and they have been shown to directly affect the interaction of another protein, HmgA1a, with heterochromatin (12). In that case, two functional AT hooks have been shown to be necessary for proper chromatin binding, and this would be consistent with the differences in subnuclear localization between the Psip1 fusion proteins in F9/3G5 and ES149 cells.

Generation of mice with disrupted *Psip1*. To investigate the phenotype of *Psip1* mutation, we generated chimeras from the ES149 cell line by blastocyst injection. Of the three chimeras obtained, two transmitted the transgene through the germ line. Heterozygous *Psip1* gene trap mouse lines from each were established in both inbred C57BL/6 and outbred MF1 backgrounds, and in most subsequent experiments mice backcrossed at least five times into each respective background were used.

The presence of the gene trap vector in genomic DNA from these mice was detected by Southern blotting or by PCR with *lacZ*-specific primers that amplify a 432-bp fragment (Fig. 3A). The endogenous *Psip1* locus was detected by amplification of an 860-bp PCR product from introns 8 and 9, which is where the gene trap construct was inserted. No amplification product was obtained from the gene-trapped locus (Fig. 3A). Southern blotting of HindIII-digested DNA with a PCR product generated from exon 9 of *Psip1* was used to confirm the genotype of homozygous gene-trapped animals. The WT locus gave a 4-kb band, while the gene-trapped locus generated a band of 8 kb (Fig. 3B).

Expression of *Psip1* during development. As gene-trapped *Psip1*-β*geo* is under the control of the endogenous promoter, we analyzed its expression during embryonic development by X-Gal staining. While no expression was detected in preimplantation embryos (0 or 2.5 dpc), ubiquitous expression was observed in heterozygous embryos at 7.5 dpc and then throughout gestation (Fig. 4A). Previous studies have shown by Northern blotting that both splice forms of *Psip1* are expressed ubiquitously in adults, although both the levels and ratios of isoforms can differ between different tissues (5).

Alternative splicing around gene trap integrations can sometimes result in the production of WT mRNAs from the trapped gene (25). We confirmed that full-length *p75*/*Psip1* mRNA is not produced from the gene-trapped locus by RT-PCR with primers downstream of the gene trap site in RNA prepared

TABLE 1. Genotypes of offspring from *Psip1*$^{+/+}$ × *Psip1*$^{+/-}$ crosses at weaning

Background	No. (%) of mice with genotype of:		Total no. of mice
	+/+	+/−	
MF1	165 (53.7)	142 (46.3)	307
C57BL/6	159 (56.2)	124 (43.8)	283

from 14.5-dpc embryos of each genotype. *p75/Psip1* mRNA is detected in RNA from +/+ or +/− embryos but absent from −/− embryos (Fig. 4B).

A recent analysis of the mouse transcriptome revealed that a large proportion of mouse genes have antisense transcripts (19). Indeed, *Psip1* partially overlaps the *Snapc3* gene on the opposite strand and the ES149 gene trap insertion site is within an intron in the 3′ untranslated region of *Snapc3* (Fig. 1A). *Snapc3* encodes a component of the snRNA-activating protein complex that recognizes snRNA promoters (13). The gene trap insertion should be spliced out of the *Snapc3* mRNA, but to ensure that the gene trap integration was not interfering with *Snapc3* expression we performed RT-PCR with primers specific for this gene. *Snapc3* mRNA was detected in both +/− and −/− embryos, so we concluded that the gene trap integration does not prevent *Snapc3* expression (Fig. 4B).

Psip1 expression was also assessed in protein extracts prepared from 14.5-dpc embryos. The p75 isoform was detected in extracts from +/+ and +/− embryos but not in samples from *Psip1*$^{-/-}$ embryos (Fig. 4C). Since the p75 isoform of Psip1 is functionally deleted in our homozygous gene-trapped mice but expression of the overlapping *Snapc3* gene does not appear to be affected, we can attribute any resultant phenotypes in the mutant mice to the loss of Psip1 function alone.

Perinatal lethality of homozygous *Psip1* mutant mice in a C57BL/6 background. In the outbred background, *Psip1*$^{+/-}$ mice were physically indistinguishable from WT littermates and were obtained at the expected frequency (Table 1). However, in an inbred (C57BL/6) background there was a small but significant deficit of heterozygous animals ($\chi^2 = 4.33$, df = 1) (Table 1).

In crosses between heterozygotes, there was no deficit of *Psip1*$^{-/-}$ embryos at various stages of development (Table 2) and they were indistinguishable from +/+ and +/− embryos. *Psip1*$^{-/-}$ pups were also present immediately after birth, in numbers compatible with normal Mendelian ratios (Table 2). However, we noticed that many pups from both C57BL/6 and MF1 breeding pairs died just after birth. The majority of these were *Psip1*$^{-/-}$ ($\chi^2 = 7.74$, df = 2) (Table 2), suggesting that there is significant perinatal lethality of *Psip1*$^{-/-}$ mice.

There were no external abnormalities in these *Psip1*$^{-/-}$ pups. Histopathology of serial sections of three −/− neonates revealed no structural abnormalities in heads, brain, thoracic organs, or abdominal organs. All had empty stomachs and

TABLE 2. Genotypes of embryos from timed matings of *Psip1*$^{+/-}$ × *Psip1*$^{+/-}$ crosses

Background and age	No. (%) of mice with genotype of:			Total no. of mice
	+/+	+/−	−/−	
C57BL/6				
12.5 dpc	5 (15)	23 (68)	6 (18)	34
16.5 dpc	9 (18)	26 (53)	14 (29)	49
Birth	9 (33)	11 (41)	7 (26)	27
MF1 + C57BL/6				
Birth (dead)[a]	5 (19)	9 (33)	13 (48)	27

[a] Pups found dead at birth from *Psip1*$^{+/-}$ × *Psip*$^{+/-}$ MF1 crosses (including those killed by the breeding pair) were recovered and genotyped.

TABLE 3. Genotypes of offspring from *Psip1*$^{+/-}$ × *Psip1*$^{+/-}$ crosses at weaning

Background	No. (%) of mice with genotype of:			Total no. of mice
	+/+	+/−	−/−	
C57BL/6, 1st backcross	32 (32)	63 (63)	5 (5)[a]	100
C57BL/6, >3 backcrosses	93 (35.9)	164 (63.7)	1 (0.4)[b]	258
MF1	182 (32.5)	351 (62.7)	27 (4.8)[c]	560

[a] One male and four females.
[b] One male.
[c] Twenty-four males and three females.

TABLE 4. Phenotypic differences found in Psip1 mutant mice in an MF1 background

Phenotype	No.[a] of mice with a genotype of:		
	+/+	+/−	−/−
Infertility[b]	Rare	Rare	5/7
Size of testes[c] (mean % ± SEM)	0.51 (0.01)	0.53 (0.02)	0.34 (0.02)
Epididymal fat pads[d]	5/5	8/8	0/7
Chronic ulcerative blepharitis[e]	Rare	Rare	20/27
Hind limb extension[f]	8/8	11/11	5/13
Normal grip strength	8/8	11/11	5/13
Brachycephaly[g]	Rare	Rare	23/27
Skeletal transformations			
Six attached ribs[h]	0/5	0/7	2/8
Eight attached ribs	1/5	2/7	0/8
Abnormal C1/C2[i]	0/2	0/4	2/4
C7 to T1[i]	0/5	0/7	4/8
T3 to T2[j]	0/3	0/4	1/4
L6 to S1[k]	0/2	0/4	3/4

[a] Unless otherwise indicated, the data are number of mice that display the observed phenotype/number of mice specifically studied for phenotype. Rare indicates that the number was not determined but the phenotype was rarely observed, if at all, during breeding of >500 offspring.
[b] Fertility of *Psip1*$^{-/-}$ mice was tested by setting up crosses between *Psip1*$^{-/-}$ males and at least two WT MF1 females. Mice were considered infertile if no offspring were obtained over a period of approximately 3 months.
[c] Size of testes was determined as the weight of both testes expressed as a percentage of body weight.
[d] See Fig. 5A.
[e] See Fig. 5D and E.
[f] See Fig. 5F.
[g] See Fig. 5G and H and 6A.
[h] See Fig. 6C.
[i] See Fig. 6D.
[j] See Fig. 6E.
[k] See Fig. 6F.

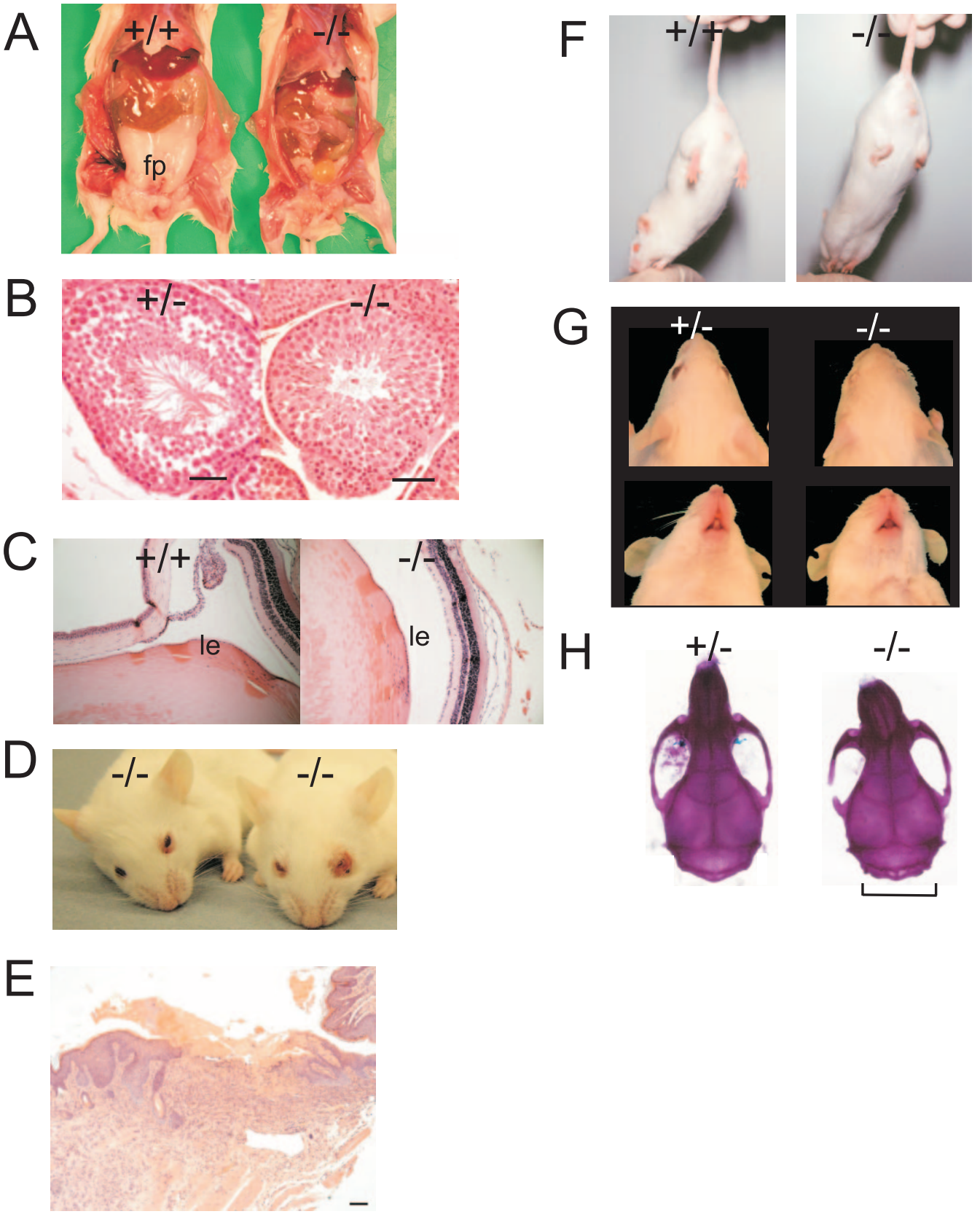

FIG. 5. Phenotypic analysis of surviving adult *Psip1*$^{-/-}$ mutant mice in the MF1 background. (A) *Psip1*$^{-/-}$ mutant mice have a reduction of intraabdominal fat, in particular, an absence of epididymal fat pads (fp), compared to their +/+ littermates. (B) H&E staining of seminiferous tubules from heterozygous (+/−) and *Psip1*$^{-/-}$ mutant mice. Both show normal-appearing basilar spermatogonia, several layers of differentiating

intestinal tracts, atrophic spleens, and scattered petechiae in the wall of the bladder near the dome. Stomachs and intestinal tracts were full in two *Psip1*$^{+/-}$ and two WT littermates which had normal spleens and no periurachal hemorrhage. The empty gastrointestinal tracts of the three null mice suggested a failure to nurse. Atrophy of the spleens was interpreted as stress related. Periurachal hemorrhage was mild and its significance questionable. On the rare occasion that litters were actually observed being born, a couple of pups (which when subsequently genotyped were *Psip1*$^{-/-}$) appeared to gasp, suggesting that they had trouble breathing, but the majority did not die immediately after birth but survived for up to the first day. As histological examination had revealed minimal structural abnormalities (including normal lungs, diaphragms, and palates) but empty stomachs, death of *Psip1*$^{-/-}$ neonates appears to be mainly the result of a failure to nurse. Inanition could be due to an inability of mutants to compete with littermates for teats, abnormal or absent nursing behavior, or rejection by the mother because of behavioral abnormalities.

Survival of a subset of homozygous mutants in a 129/Ola-C57BL/6 hybrid or outbred MF1 background. Only one homozygous animal in the C57BL/6 background survived to weaning at 4 weeks (Table 3). From *Psip1*$^{+/-}$ intercrosses of mice from either the first backcross into the C57BL/6 background or in the outbred MF1 background, the majority of homozygous mutant offspring also died just after birth and showed a failure to nurse. However, of those that were present after weaning ($\chi^2 = 21.3$ and 121.8) (Table 3), the majority then survived for >6 months, although a number of subtle differences between *Psip1*$^{-/-}$ adults and their WT and heterozygous littermates were detected.

Psip1$^{-/-}$ mice were very lean, with reduced intraabdominal fat and a complete absence of epididymal fat pads (Table 4 and Fig. 5A). Most (24 out of 27) of the surviving homozygotes in the MF1 background were male. These had low fertility; the majority of those tested failed to produce any offspring, and those that did only produced one or two litters. They had small testes compared to their +/+ and +/− littermates, even when corrected for body weight (Table 4). Testicular histopathology did not reveal any differences in the appearance of seminiferous tubules or the Leydig cell-containing interstitium between *Psip1*$^{-/-}$ and WT mice. All stages of spermiogenesis were present (Fig. 5B).

Eye phenotypes in homozygous mutant mice. Psip1 (LEDGF) was originally described as a growth factor produced by lens epithelial cells and has been reported to function in the survival of lens epithelial cells (34). Immunostaining showed that, in *Psip1*$^{+/+}$ mice, p75/Psip1 was expressed in nuclei of lens epithelial cells and in cells of the cornea, sclera, uvea, and retina (data not shown). However, after H&E staining, the lens epithelium appeared to be normal in *Psip1*$^{-/-}$ mice, suggesting that, in vivo, Psip1 (Ledgf) does not function to promote the survival or growth of the lens epithelium (Fig. 5C).

TABLE 5. Performance of WT and *Psip1* mutant mice in an open-field test

Genotype	No. of animals	Total no. of squares visited	% of inner-square visits	No. of rearings
+/+	10	208 (30.7)[a]	16.9 (4.3)	15.5 (3.5)
+/−	16	172.3 (19.5)	11.5 (2.6)	16.5 (1.7)
−/−	9	49 (18.7)[b]	14.7 (4.6)	2.7 (1.7)[b]

[a] Mean (standard error of the mean).
[b] $P < 0.05$ compared to +/+ and +/− mice by Dunnett's multiple comparison.

The majority of *Psip1*$^{-/-}$ mice did develop persistent inflammation of the eyelids of one or both orbits (Fig. 5D), which was rarely observed in *Psip1*$^{+/-}$ or WT littermates. This varied in severity but worsened with age. Histopathology confirmed this to be chronic ulcerative blepharitis with sparing of the adjacent conjunctiva. The epidermis was ulcerated and covered with adherent fibrin plaque. Chronic mixed inflammatory cells infiltrated the dermis. There were no structural abnormalities to explain this proclivity (Fig. 5E).

Motor and behavioral abnormalities in *Psip1* mutants. Survivor *Psip1*$^{-/-}$ mice and their +/+ and +/− littermates were tested for basic motor functions. Hind limb extension and splaying of toes are natural reflexes for a mouse suspended by its tail, but *Psip1*$^{-/-}$ mice had a tendency to clench their toes and their hind limbs to their bodies (Table 4 and Fig. 5F). This became more pronounced with age. *Psip1*$^{-/-}$ mice also had reduced grip strength compared to littermates (Table 4).

In an open-field test, the total number of squares visited by *Psip1*$^{-/-}$ mice was significantly reduced (Table 5). A one-way analysis of variance [$(F2,32) = 10.62$ and $P = 0.003$] demonstrated a highly significant difference between the genotypes. Post hoc analysis by Dunnett's test showed that the significance lies in homozygous mutant mice being significantly different ($P < 0.05$) from both WT and heterozygous mice. There was no difference in these parameters between +/+ and +/− mice. Decreased movement by *Psip1*$^{-/-}$ mice could be because they find it difficult or painful to move or because they are anxious or inhibited. The latter explanation is less likely, as the proportions of crossings in the more anxiogenic inner zones are similar among all of the genotypes (Table 5). Furthermore, rearing on the hind legs is also significantly reduced, which may reflect the general problems observed with movement in *Psip1*$^{-/-}$ mice.

The motor abnormalities of *Psip1*$^{-/-}$ mice will affect behavior and could explain why the majority of mutants fail to nurse. They may either have difficulty in, or be uninterested in, feed-

spermatocytes, and maturing spermatids at the lumen. Bars, 50 μm. (C) H&E staining of eyes from WT (+/+) and *Psip1*$^{-/-}$ mutant mice showing a normal lens epithelium (le). (D) Chronic ulcerative blepharitis in *Psip1*$^{-/-}$ mutant mice. The mouse on the left is 2 months old; the right eye is asymptomatic, and the left eye shows mild symptoms. The mouse on the right is 4 months old; symptoms in the right eye are mild, and those in the left eye are severe. (E) H&E staining of the eyelid of a *Psip1*$^{-/-}$ mutant mouse showing ulcerated epidermis covered with adherent fibrin plaque. The adjacent intact epidermis is hyperplastic, and chronic mixed inflammatory cells have infiltrated the dermis. Bar, 100 μm. (F) *Psip1*$^{-/-}$ mutant mice clench their hind limbs, in contrast to the hind limb extension of +/+ mice. (G) *Psip1*$^{-/-}$ mutant mice have brachycephaly with broad, shortened faces and jaws. (H) Alizarin red-alcian blue staining of skulls shows that the cranial bones and nasal process are broader and shorter in *Psip1*$^{-/-}$ mutant mice compared to those of +/− (and +/+) mice.

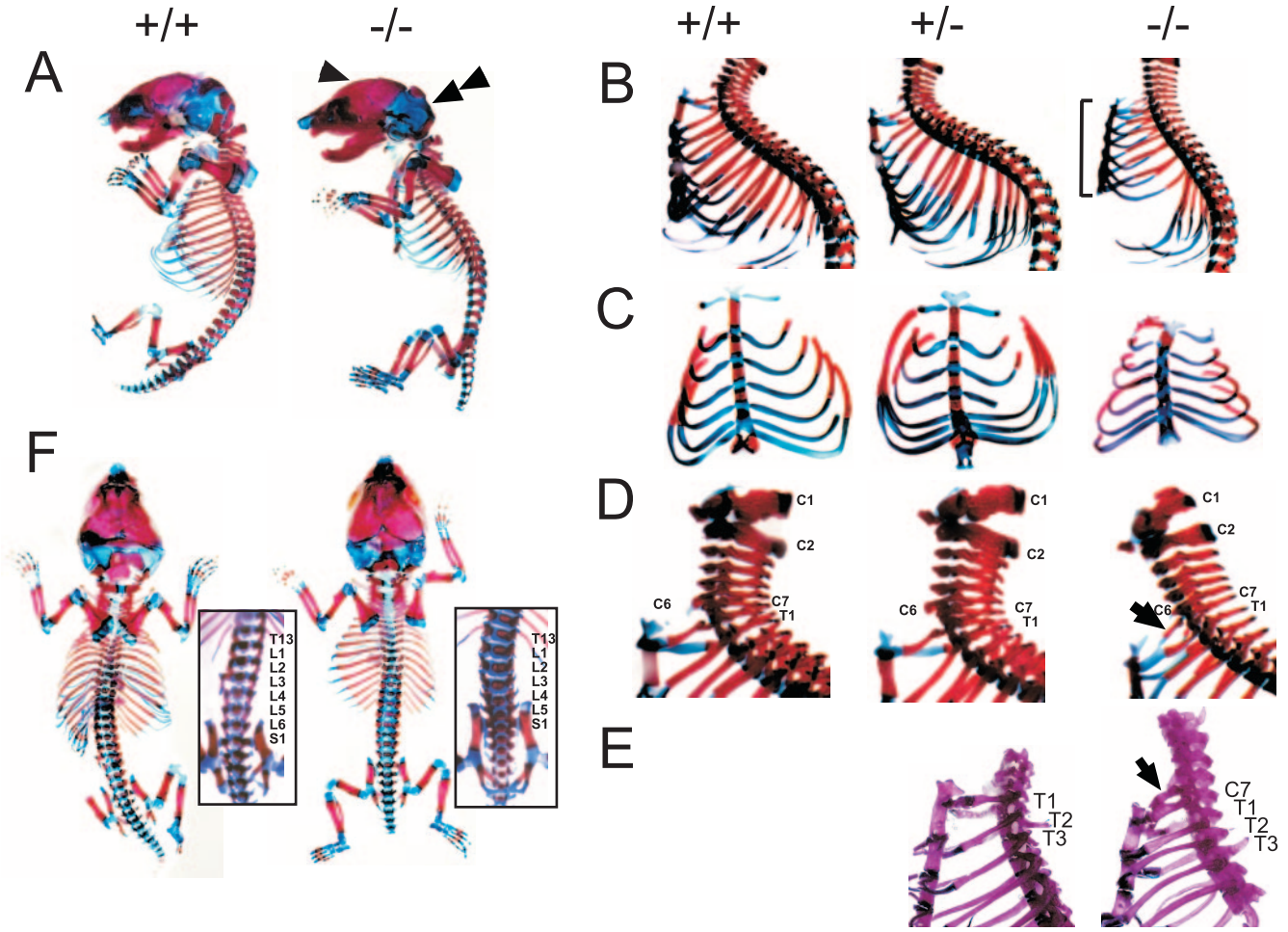

FIG. 6. Alizarin red-alcian blue staining reveals craniofacial and skeletal abnormalities in *Psip1*$^{-/-}$ mutant mice. (A) Staining of +/+ and *Psip1*$^{-/-}$ mutant MF1 newborn skeletons. −/− pups have domed skulls (arrowheads) and reduced interparietal, exoccipital, and supraoccipital bones (double arrowheads). (B) *Psip1*$^{-/-}$ mutant pups lack physiological curvature of the spine and have a small rib cage and a short sternum, compared to +/+ and +/− littermates. (C) Dissected rib cages from C57BL/6 +/+, +/−, and −/− newborn pups. (D) Cervical region, showing misshapen C1 and C2 and an incomplete ectopic rib (arrow) from C7 that is fused with the cartilage of T1. (E) Adult skeletons showing an incomplete ectopic rib (arrowed) from C7 unilaterally fused with T1 and a prominent spinous process, characteristic for T2, incorrectly associated with T3 in a *Psip1*$^{-/-}$ mutant animal. (F) +/+ and −/− MF1 newborn skeletons showing a reduced number of lumbar vertebrae and transformation of L6 into S1.

ing, or they may be rejected by their mothers because of their abnormal movement or behavior.

Brachycephaly and skeletal homeotic transformations in *Psip1* mutants. Surviving *Psip1*$^{-/-}$ mice tend to have broad, shortened faces and jaws and often a slightly hunched appearance (Fig. 5G). Alizarin red-alcian blue staining of skulls showed no obvious differences in the sutures or in the composition of the skull bones but that the cranial bones and nasal process are broader and shorter in the homozygous mutants compared to those of WT and heterozygous mice (Fig. 5H). In particular, the occipital bone at the back of the skull appears to be flatter and broader. Some mutants had highly domed craniums. Craniofacial abnormalities characterized by a domed skull and a reduction in the extent of the interparietal, exoccipital, and supraoccipital bones were also seen in −/− newborns (Fig. 6A). The skulls of *Psip1*$^{-/-}$ newborns were often more fragile than those of WT littermates during staining, suggesting that the bones of the roof of the skull may be thinner. No difference compared with WT animals was detected in the bones of the base of the skull.

Skeletal abnormalities were also found in *Psip1*$^{-/-}$ newborns and adults (Fig. 6), although the penetrance was incomplete and variable (Table 4). For example, the spine was less curved and the rib cage smaller, with the sternum sitting closer to the backbone (Fig. 6B). This is due to a short sternum and short and fewer ribs (6 connected to the sternebrae, compared to the usual 7, resulting in 12 in total, compared to the usual 13) (Fig. 6C). Furthermore, the ribs are attached asymmetrically and the alternating pattern of cartilage and bone up the sternebrae is disorganized.

Some −/− animals exhibited skeletal alterations along the anterior-posterior axis that were consistent with homeotic transformations. Figure 6D highlights the abnormally shaped first and second cervical vertebrae (C1 and C2) of *Psip1*$^{-/-}$ pups. As seen in some of the surviving *Psip1*$^{-/-}$ adult mice, the seventh cervical vertebra (C7) had an incomplete ectopic rib

that fused with the cartilage of the first thoracic rib (T1), suggesting a posterior homeotic transformation of C7 to T1. A prominent spinous process, characteristic for the second thoracic vertebra (T2) was incorrectly associated with the third thoracic vertebra (T3) in one adult mutant, suggesting an anterior shift in the identity of T3 to T2 (Fig. 6E).

Most *Psip1*$^{-/-}$ mice also show homeotic transformations in the lumbar region, with only five lumbar vertebrae (Fig. 6F, inset), indicating a posterior transformation of L6 to sacral vertebra 1 (S1).

Evidence for upregulation of *Hox* genes in the absence of Psip1 (LEDGF). Posterior transformation of cervical vertebra C7 to thoracic vertebra T1 is a phenotype also seen in mice mutant for *Hoxa4* (14), *Hoxa5* (18), and *Hoxa6* (20). Therefore, Psip1 may be involved either in the control of *Hox* gene expression or as a downstream effector of Hox function.

To find evidence for *Hox* gene deregulation in the absence of Psip1, mouse embryonic fibroblasts (MEFs) were derived from the bodies of genotyped embryos at 11.5 dpc, a stage when there appears to be widespread *Psip1* expression (Fig. 4A). RNAs prepared from passage 5 WT and *Psip1*$^{-/-}$ MEFs were analyzed for the expression of *Hox* genes by RT-PCR. No expression of *Hoxa9*, *Hoxa13*, *Hoxb1*, *Hoxb8*, or *Hoxb13* was detected in either WT or mutant MEFs. Expression of *Hoxa6*, *Hoxb3*, *Hoxb5*, *Hoxb6*, *Hoxb7*, and *Hoxb9* was detected, but there was no obvious difference between the levels of expression of these genes in WT and mutant MEFs (data not shown).

However, analysis of the results of transcriptional profiling of human embryonic kidney (HEK) 293 cells subjected to small interfering (siRNA) for p75/PSIP1 does support the hypothesis that PSIP1 can be involved in the regulation of *HOX* gene expression (5). Compared to control cells (with scrambled siRNAs), global levels of gene expression were unaltered in knockdown cells (mean ratio of p75/PSIP1 siRNA expression to scrambled control expression = 0.96) (http://www.ncbi.nlm.nih.gov/geo/; accession no. GSE3485). For each probe's signal deemed "present" in this analysis, we calculated the mean value and standard deviation across the four knockdown and the four control arrays. Probes significantly ($P < 0.01$) up- or down-regulated in the knockdown were then identified with an unpaired *t* test. This gave 358 significantly up-regulated and 479 down-regulated probes, mapping to 268 and 342 Ensembl genes, respectively. Among these up-regulated genes were *HOXA5*, *HOXA6 HOXA9*, *HOXA10*, and *HOXA13*. Genes from other *HOX* clusters were generally found not to be expressed in HEK 293 cells, but *HOXD8* was found to be down-regulated in the knockdown cells. Although established by adenovirus transformation of primary HEK cells, subsequent microarray analysis has indicated that HEK 293 cells are of neuronal origin (31). These data therefore indicate that loss of PSIP1 can lead to dysregulation of *HOX* genes in some cell types.

DISCUSSION

We have used gene trap mutagenesis to investigate the biological function of *Psip1* in the mouse. Psip1 is a ubiquitous chromatin-associated protein, isoforms of which have been variously implicated in transcriptional regulation, mRNA splicing, and cell survival in vitro (7, 8, 32). Gene trap insertion into *Psip1* abrogates expression of both isoforms of the normal Psip1 protein (Fig. 1 and 4), so we cannot attribute mutant phenotypes to one or other of the isoforms. Psip1 is expressed throughout mouse embryonic development, and even though the gene-trapped Psip1-βgeo fusion protein lacks important functional and conserved domains (Fig. 1), the mutant phenotype is only manifested after birth. Therefore, full-length Psip1 is not essential for the survival of cells or for their proliferation.

Psip1 (LEDGF) was originally described as a growth factor produced by lens epithelial cells and has been reported to function in the survival of lens epithelial cells in vitro (34). It has also been suggested to play a protective role against stress in corneal keratinocytes (21). We found that p75/Psip1 is expressed in nuclei of lens epithelial cells and in cells of the cornea, sclera, uvea, and retina. However, the lens epithelium and cornea appear to be normal in *Psip1*$^{-/-}$ mutant mice (Fig. 5C), suggesting that, in vivo, Psip1 does not function to promote the survival or growth of the lens epithelium or cornea.

The most dramatic aspect of the *Psip1*$^{-/-}$ phenotype is that the majority of pups died during the first day after birth. However, a subset of *Psip1*$^{-/-}$ mutant mice survived and these displayed skeletal abnormalities reminiscent of homeotic transformations. The ectopic ribs seen on cervical vertebra C7 are consistent with a posterior homeotic transformation to thoracic vertebra T1 (Fig. 6D and E), and this is also seen in mice with *Hoxa4* (14), *Hoxa5* (18), and *Hoxa6* (20) mutations. *Hoxc4* mutant animals also have an abnormal C7 vertebra, but in this case only rib heads are formed (30). Also, similar to *Hoxc4* mutants, the surviving *Psip1*$^{-/-}$ mutant animals have a process on T3, which is normally associated with T2, suggestive of an anterior T3-T2 transformation (Fig. 6E).

We therefore considered the possibility that Psip1 is involved either in the control of *Hox* gene expression or as a downstream effector of Hox function. Although we found no evidence for misregulation of *Hox* gene expression in MEFs derived from *Psip1*$^{-/-}$ embryos, we did find it in a microarray data set of transcriptional profiling of HEK 293 cells subjected to siRNA for p75/PSIP1 (5). Almost 2% of the genes most significantly ($P < 0.01$) up-regulated in the knockdown cells were genes from the 5′ end of the *HOXA* cluster (*HOXA5*, *HOXA6 HOXA9*, *HOXA10*, and *HOXA13*). The upregulation of these "posterior" members of the *HOXA* cluster in cultured cells deficient in p75/PSIP1 would be consistent with the posterior homeotic transformations in our *Psip1*$^{-/-}$ mice.

As well as a role in transcriptional regulation, the p52 isoform of Psip1 has been shown to interact with the splicing factor SF2 and to modulate its activity (9). It is therefore intriguing that animals heterozygous for mutation in an essential splicing factor, SF3b1, a component of the U2 snRNP, showed posterior homeotic transformations similar to those seen in *Psip1*$^{-/-}$ mutant mice, including ectopic ribs on C7 and L6-to-S1 transformation (17).

We suggest that Psip1 may have an unexpected function in the transcriptional repression of homeotic genes and the specification of identity along the axial skeleton. In this regard, it is interesting that human PSIP1 (LEDGF) is found as a translocation-induced fusion partner with NUP98 in acute and chronic myeloid leukemias (11, 15). In these cases, the part of PSIP1 that is retained in the fusion protein (beyond exon 7) is the part that is missing in our mutant mice. The other recur-

rent leukemia-associated fusion partners with NUP98 are encoded by the *HOX* genes themselves (1). Further investigation of the interactions between *Hox* genes and Psip1 may help to elucidate the molecular etiology of these leukemias. Lastly, knocking minigenes for the different Psip1 isoforms back into our mutant mice may help to dissect the different functions of the alternatively spliced isoforms of Psip1.

ACKNOWLEDGMENTS

H.G.S. was supported by fellowships from European Molecular Biology Organization and the Association for International Cancer Research. W.A.B. is a Centennial Fellow of the James S. McDonnell Foundation, and this work was supported by the Medical Research Council, UK, and in part by FP6 through funding for the Epigenome Network of Excellence under contract LSHG-CT-2004-503433.

We thank Phillipe Gautier (MRC HGU) for help with the bioinformatics, Sandy Bruce for photography, and Bob Hill for critical reading of the manuscript. We are grateful to Toshimichi Shinohara (Boston, MA) for the human LEDGF cDNA.

REFERENCES

1. **Abramovich, C., N. Pineault, H. Ohta, and R. K. Humphries.** 2005. Hox genes: from leukemia to hematopoietic stem cell expansion. Ann. N. Y. Acad. Sci. **1044:**109–116.
2. **Chen, T., N. Tsujimoto, and E. Li.** 2004. The PWWP domain of Dnmt3a and Dnmt3b is required for directing DNA methylation to the major satellite repeats at pericentric heterochromatin. Mol. Cell. Biol. **24:**9048–9058.
3. **Cherepanov, P., A. L. Ambrosio, S. Rahman, T. Ellenberger, and A. Engelman.** 2005. Structural basis for the recognition between HIV-1 integrase and transcriptional coactivator p75. Proc. Natl. Acad. Sci. USA **102:**17308–17313.
4. **Cherepanov, P., E. Devroe, P. A. Silver, and A. Engelman.** 2004. Identification of an evolutionarily conserved domain in human lens epithelium-derived growth factor/transcriptional co-activator p75 (LEDGF/p75) that binds HIV-1 integrase. J. Biol. Chem. **279:**48883–48892.
5. **Ciuffi, A., M. Llano, E. Poeschla, C. Hoffmann, J. Leipzig, P. Shinn, J. R. Ecker, and F. Bushman.** 2005. A role for LEDGF/p75 in targeting HIV DNA integration. Nat. Med. **11:**1287–1289.
6. **Emiliani, S., A. Mousnier, K. Busschots, M. Maroun, B. Van Maele, D. Tempe, L. Vandekerckhove, F. Moisant, L. Ben Slama, M. Witvrouw, F. Christ, J. C. Rain, C. Dargemont, Z. Debyser, and R. Benarous.** 2005. Integrase mutants defective for interaction with LEDGF/p75 are impaired in chromosome tethering and HIV-1 replication. J. Biol. Chem. **280:**25517–25523.
7. **Ganapathy, V., T. Daniels, and C. A. Casiano.** 2003. LEDGF/p75: a novel nuclear autoantigen at the crossroads of cell survival and apoptosis. Autoimmun. Rev. **2:**290–297.
8. **Ge, H., Y. Si, and R. G. Roeder.** 1998. Isolation of cDNAs encoding novel transcription coactivators p52 and p75 reveals an alternate regulatory mechanism of transcriptional activation. EMBO J. **17:**6723–6729.
9. **Ge, H., Y. Si, and A. P. Wolffe.** 1998. A novel transcriptional coactivator, p52, functionally interacts with the essential splicing factor ASF/SF2. Mol. Cell **2:**751–759.
10. **Ge, Y. Z., M. T. Pu, H. Gowher, H. P. Wu, J. P. Ding, A. Jeltsch, and G. L. Xu.** 2004. Chromatin targeting of de novo DNA methyltransferases by the PWWP domain. J. Biol. Chem. **279:**25447–25454.
11. **Grand, F. H., P. Koduru, N. C. Cross, and S. L. Allen.** 2005. NUP98-LEDGF fusion and t(9;11) in transformed chronic myeloid leukemia. Leuk. Res. **29:**1469–1472.
12. **Harrer, M., H. Luhrs, M. Bustin, U. Scheer, and R. Hock.** 2004. Dynamic interaction of HMGA1a proteins with chromatin. J. Cell Sci. **117:**3459–3471.
13. **Henry, R. W., B. Ma, C. L. Sadowski, R. Kobayashi, and N. Hernandez.** 1996. Cloning and characterization of SNAP50, a subunit of the snRNA-activating protein complex SNAPc. EMBO J. **15:**7129–7136.
14. **Horan, G. S., K. Wu, D. J. Wolgemuth, and R. R. Behringer.** 1994. Homeotic transformation of cervical vertebrae in Hoxa-4 mutant mice. Proc. Natl. Acad. Sci. USA **91:**12644–12648.
15. **Hussey, D. J., S. Moore, M. Nicola, and A. Dobrovic.** 2001. Fusion of the NUP98 gene with the LEDGF/p52 gene defines a recurrent acute myeloid leukemia translocation. BMC Genet. **2:**20.
16. **Isaac, C., K. L. Marsh, W. A. Paznekas, J. Dixon, M. J. Dixon, E. W. Jabs, and U. T. Meier.** 2000. Characterization of the nucleolar gene product, treacle, in Treacher Collins syndrome. Mol. Biol. Cell **11:**3061–3071.
17. **Isono, K., Y. Mizutani-Koseki, T. Komori, M. S. Schmidt-Zachmann, and H. Koseki.** 2005. Mammalian polycomb-mediated repression of Hox genes requires the essential spliceosomal protein Sf3b1. Genes Dev. **19:**536–541.
18. **Jeannotte, L., M. Lemieux, J. Charron, F. Poirier, and E. J. Robertson.** 1993. Specification of axial identity in the mouse: role of the Hoxa-5 (Hox1.3) gene. Genes Dev. **7:**2085–2096.
19. **Katayama, S., Y. Tomaru, T. Kasukawa, K. Waki, M. Nakanishi, M. Nakamura, H. Nishida, C. C. Yap, M. Suzuki, J. Kawai, H. Suzuki, P. Carninci, Y. Hayashizaki, C. Wells, M. Frith, T. Ravasi, K. C. Pang, J. Hallinan, J. Mattick, D. A. Hume, L. Lipovich, S. Batalov, P. G. Engstrom, Y. Mizuno, M. A. Faghihi, A. Sandelin, A. M. Chalk, S. Mottagui-Tabar, Z. Liang, B. Lenhard, and C. Wahlestedt.** 2005. Antisense transcription in the mammalian transcriptome. Science **309:**1564–1566.
20. **Kostic, D., and M. R. Capecchi.** 1994. Targeted disruptions of the murine Hoxa-4 and Hoxa-6 genes result in homeotic transformations of components of the vertebral column. Mech. Dev. **46:**231–247.
21. **Kubo, E., N. Fatma, P. Sharma, T. Shinohara, L. T. Chylack, Jr., Y. Akagi, and D. P. Singh.** 2002. Transactivation of involucrin, a marker of differentiation in keratinocytes, by lens epithelium-derived growth factor (LEDGF). J. Mol. Biol. **320:**1053–1063.
22. **Llano, M., S. Delgado, M. Vanegas, and E. M. Poeschla.** 2004. Lens epithelium-derived growth factor/p75 prevents proteasomal degradation of HIV-1 integrase. J. Biol. Chem. **279:**55570–55577.
23. **Maertens, G., P. Cherepanov, W. Pluymers, K. Busschots, E. De Clercq, Z. Debyser, and Y. Engelborghs.** 2003. LEDGF/p75 is essential for nuclear and chromosomal targeting of HIV-1 integrase in human cells. J. Biol. Chem. **278:**33528–33539.
24. **Maurer-Stroh, S., N. J. Dickens, L. Hughes-Davies, T. Kouzarides, F. Eisenhaber, and C. P. Ponting.** 2003. The Tudor domain 'Royal Family': Tudor, plant Agenet, Chromo, PWWP and MBT domains. Trends Biochem. Sci. **28:**69–74.
25. **McClive, P., G. Pall, K. Newton, M. Lee, J. Mullins, and L. Forrester.** 1998. Gene trap integrations expressed in the developing heart: insertion site affects splicing of the PT1-ATG vector. Dev. Dyn. **212:**267–276.
26. **Newton, K., E. Petfalski, D. Tollervey, and J. F. Caceres.** 2003. Fibrillarin is essential for early development and required for accumulation of an intron-encoded small nucleolar RNA in the mouse. Mol. Cell. Biol. **23:**8519–8527.
27. **Nishizawa, Y., J. Usukura, D. P. Singh, L. T. Chylack, Jr., and T. Shinohara.** 2001. Spatial and temporal dynamics of two alternatively spliced regulatory factors, lens epithelium-derived growth factor (ledgf/p75) and p52, in the nucleus. Cell Tissue Res. **305:**107–114.
28. **Ochs, R. L., Y. Muro, Y. Si, H. Ge, E. K. Chan, and E. M. Tan.** 2000. Autoantibodies to DFS 70 kd/transcription coactivator p75 in atopic dermatitis and other conditions. J. Allergy Clin. Immunol. **105:**1211–1220.
29. **Patton, J. T., and M. H. Kaufman.** 1995. The timing of ossification of the limb bones, and growth rates of various long bones of the fore and hind limbs of the prenatal and early postnatal laboratory mouse. J. Anat. **186**(Pt. 1)**:** 175–185.
30. **Saegusa, H., N. Takahashi, S. Noguchi, and H. Suemori.** 1996. Targeted disruption in the mouse Hoxc-4 locus results in axial skeleton homeosis and malformation of the xiphoid process. Dev. Biol. **174:**55–64.
31. **Shaw, G., S. Morse, M. Ararat, and F. L. Graham.** 2002. Preferential transformation of human neuronal cells by human adenoviruses and the origin of HEK 293 cells. FASEB J. **16:**869–871.
32. **Shinohara, T., D. P. Singh, and N. Fatma.** 2002. LEDGF, a survival factor, activates stress-related genes. Prog. Retinal Eye Res. **21:**341–358.
33. **Singh, D. P., E. Kubo, Y. Takamura, T. Shinohara, A. Kumar, L. T. Chylack, Jr., and N. Fatma.** 2006. DNA binding domains and nuclear localization signal of LEDGF: contribution of two helix-turn-helix (HTH)-like domains and a stretch of 58 amino acids of the N-terminal to the trans-activation potential of LEDGF. J. Mol. Biol. **355:**379–394.
34. **Singh, D. P., N. Ohguro, T. Kikuchi, T. Sueno, V. N. Reddy, K. Yuge, L. T. Chylack, Jr., and T. Shinohara.** 2000. Lens epithelium-derived growth factor: effects on growth and survival of lens epithelial cells, keratinocytes, and fibroblasts. Biochem. Biophys. Res. Commun. **267:**373–381.
35. **Sutherland, H. G., G. K. Mumford, K. Newton, L. V. Ford, R. Farrall, G. Dellaire, J. F. Caceres, and W. A. Bickmore.** 2001. Large-scale identification of mammalian proteins localized to nuclear sub-compartments. Hum. Mol. Genet. **10:**1995–2011.
36. **Turlure, F., G. Maertens, S. Rahman, P. Cherepanov, and A. Engelman.** 2006. A tripartite DNA-binding element, comprised of the nuclear localization signal and two AT-hook motifs, mediates the association of LEDGF/p75 with chromatin in vivo. Nucleic Acids Res. **34:**1663–1675.
37. **Vanegas, M., M. Llano, S. Delgado, D. Thompson, M. Peretz, and E. Poeschla.** 2005. Identification of the LEDGF/p75 HIV-1 integrase-interaction domain and NLS reveals NLS-independent chromatin tethering. J. Cell Sci. **118:**1733–1743.
38. **Wu, X., T. Daniels, C. Molinaro, M. B. Lilly, and C. A. Casiano.** 2002. Caspase cleavage of the nuclear autoantigen LEDGF/p75 abrogates its pro-survival function: implications for autoimmunity in atopic disorders. Cell Death Differ. **9:**915–925.